J Fluoresc (2015) 25:1437–1447
DOI 10.1007/s10895-015-1634-x

ORIGINAL ARTICLE

Pyridoxal Based Fluorescent Chemosensor for Detection of Copper(II) in Solution With Moderate Selectivity and Live Cell Imaging

Senjuti Mandal[1] · **Sushil Kumar Mandal**[2] · **Anisur Rahman Khuda-Bukhsh**[2] · **Sanchita Goswami**[1]

Received: 11 June 2015 / Accepted: 26 July 2015 / Published online: 6 August 2015

Abstract A pyridoxal-based fluorescent probe **HL** was synthesized for the detection of Cu^{2+} in methanol with moderate selectivity. Upon addition of Cu^{2+}, to the solution of the probe in methanol exhibited a remarkable change in emission at 500 nm. With the limit of detection of 10 μM, the probe could well meet the recommended (less than 32 μM in drinking water) of the World Health Organization (WHO). The intracellular Cu^{2+} imaging behaviour of **HL** was carried out on HeLa cells.

Keywords Copper(II) · Schiff base · Pyridoxal · Fluorescence quenching · Biological study

Introduction

Copper is an essential trace element that is widely distributed in animal and plant tissues [1, 2]. It also acts as a cofactor for a number of metalloenzymes such as catalase, peroxidase and cytochrome oxidase to facilitate enzyme function [3]. Copper ion is physiologically essential for human heath as it plays important roles in bone formation, connective tissue development and cellular respiration and is also a fundamental nutrient at low amounts, <0.9 mg/day for normal adults [4]. However, on the other hand, excessive amounts of copper can result in severe diseases, for example, eczema, damage of kidneys, neurodegenerative diseases etc. [5, 6]. The allowed concentration of copper ion in drinking water is less than 2 mg L^{-1} (32 μM), according to guidelines for drinking-water quality of the World Health Organization (WHO) [7] and excessive copper is not removed by conventional water treatment processes. Therefore, in environment as well as health monitoring, the detection of Cu^{2+} is undoubtedly important. As a result, various analytical techniques for Cu^{2+} detection have been developed such as by atomic absorption/emission spectroscopy [8], inductively coupled plasma mass spectrometry (ICP-MS) [9], and capillary electrophoresis [10]. However, all of these methods require expensive and sophisticated instruments combined with complicated sample pretreatment and therefore impractical for a real-time experiment. Recently, metal-selective fluorescent chemosensors have attracted intense attention for their simple, economical and real-time tracking of metal ions in environmental samples [11, 12] Cu^{2+} is a typical ion that leads to decreased fluorescent emissions owing to quenching of the fluorescence by mechanisms inherent to the paramagnetic species [13, 14].

Again, the luminescence properties of pyridoxal are well known [15]. Therefore, we intended to explore the potential of pyridoxal containing compounds as effective sensing devices. Pyridoxal moiety imparts a physiological feasibility as it is the biologically active form of vitamin B_6, pyridoxal 5- phosphate (PLP) and a versatile enzyme cofactor responsible for amino acid metabolism in organisms ranging from bacteria to human [16–50]. Several metal complexes of Schiff bases derived from pyridoxal and amino acids/polyamines have been reported [51–62]. Recently, a new Schiff base was generated by condensing equimolar pyridoxal with 2-aminoethyl pyridine and its vanadium and copper complexes were prepared [63, 64].

✉ Sanchita Goswami
sgchem@caluniv.ac.in

[1] Department of Chemistry, University of Calcutta, 92, A. P. C. Road, Kolkata 700009, India

[2] Cytogenetics and Molecular Biology Laboratory, Department of Zoology, University of Kalyani, Kalyani 741235, India

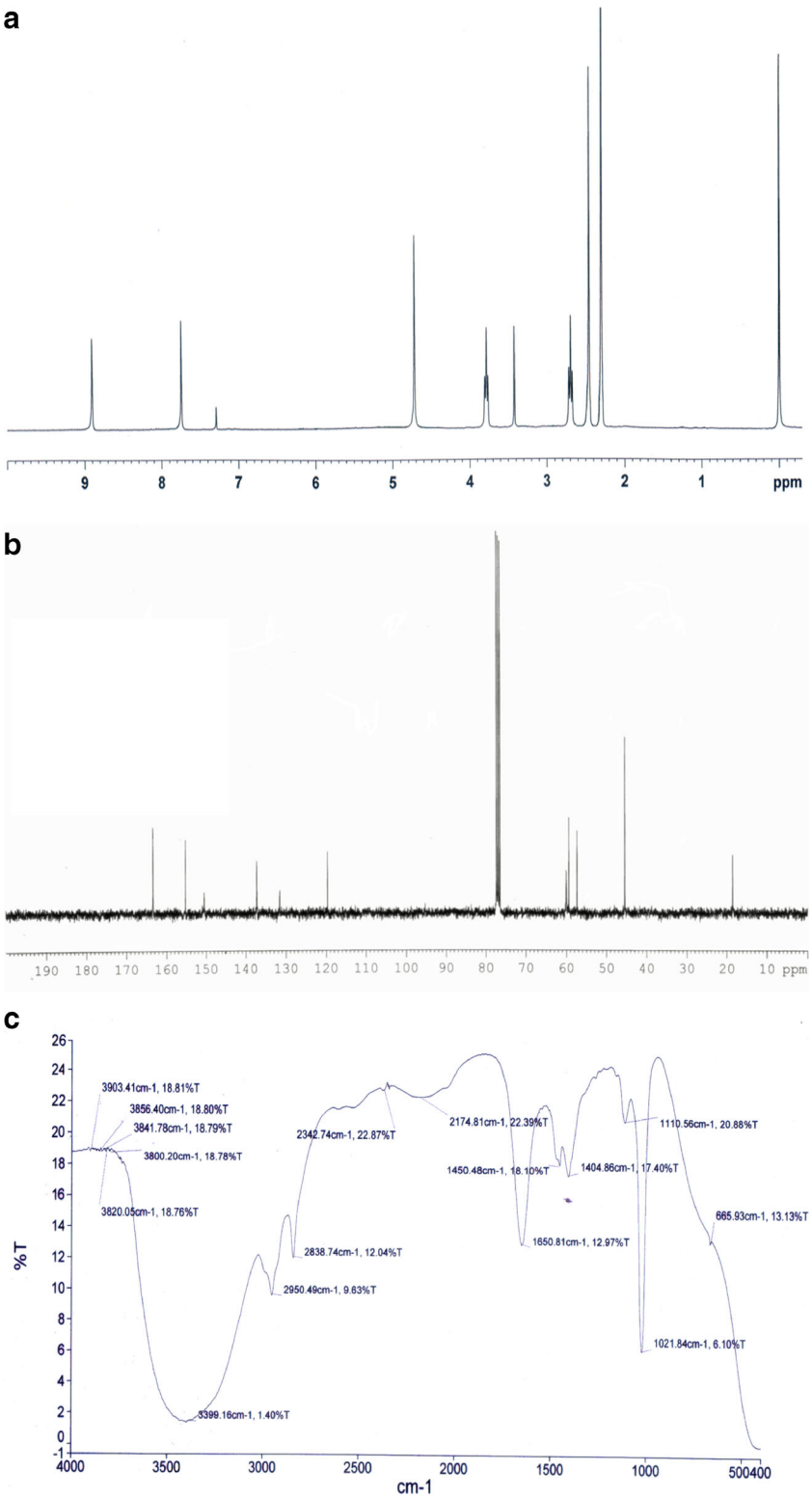

Fig. 1 **a** ^{1}H NMR, **b** ^{13}C NMR in $CDCl_3$ and **c** FTIR spectra of **HL**

The work presented herein is part of an extensive experimental study designed to explore the potential of pyridoxal Schiff bases to act as effective sensing material [64]. In this paper, we report on the fluorescence quenching behaviour of **HL** with moderate selectivity towards Cu^{2+} in methanol (where, **HL**=[((2-(dimethylamino)ethylimino)methyl)-5-(hydroxymethyl)-2-methylpyridin-3-ol]. Biological study was carried out with human cervical cancer cells of HeLa cell line.

Scheme 1 The schematic representation of preparation of **HL** and its copper (II) complexes

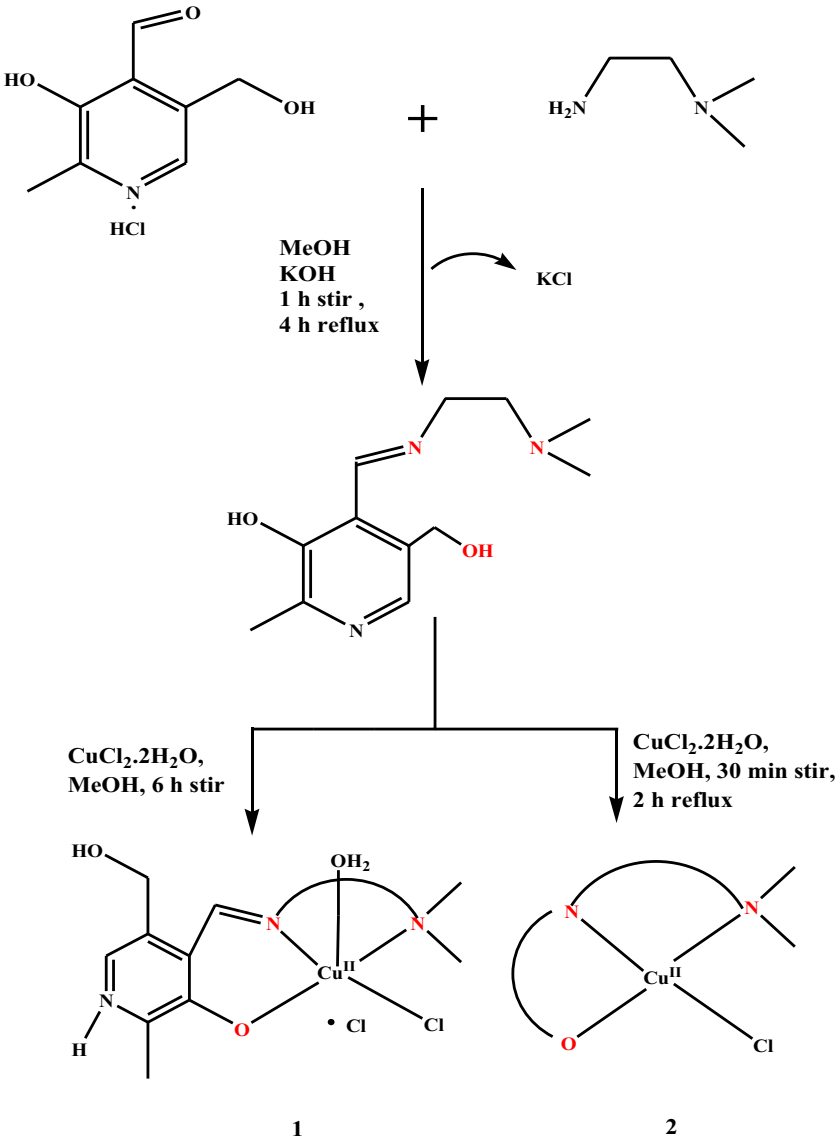

Fig. 2 Electronic spectra of **HL** (10^{-4} M) in methanol

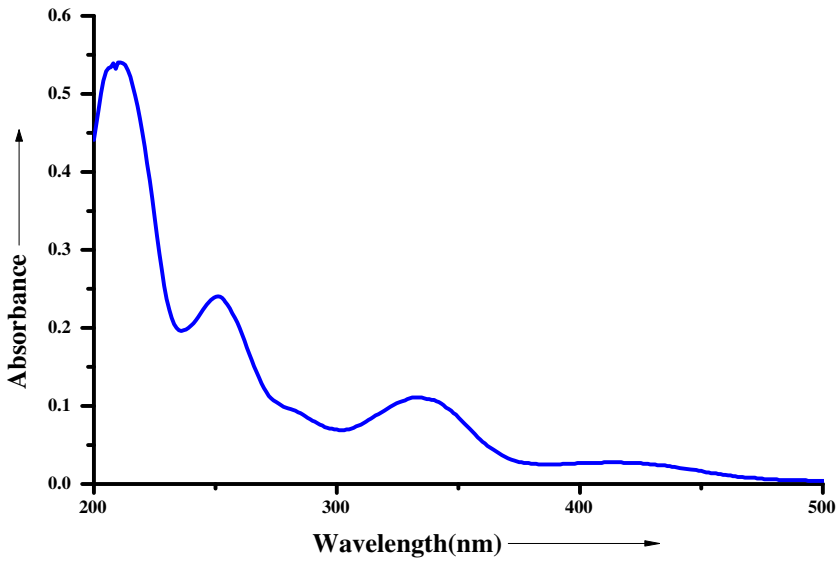

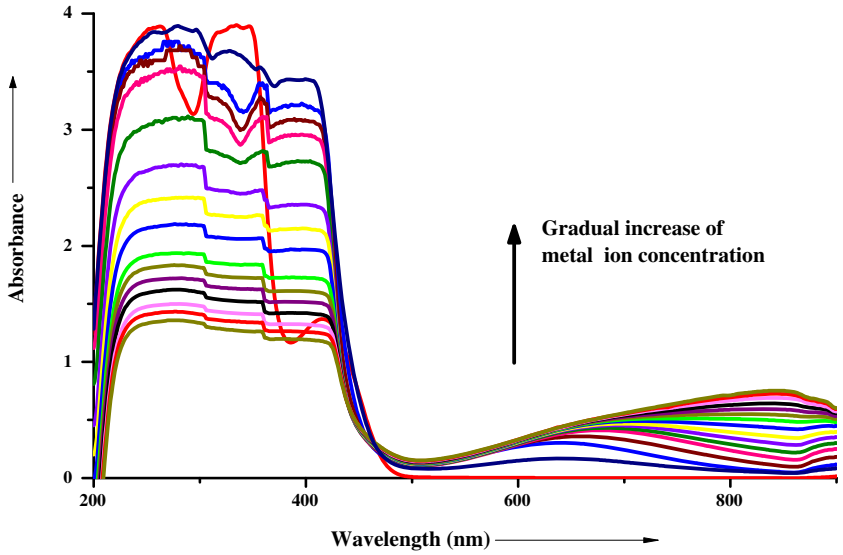

Fig. 3 UV–vis spectral change of **HL** (10^{-4} M) upon the addition of Cu^{2+} in methanol at 25 °C, [stock solution of Cu^{2+}]=0.5 M

Experimental Details

Materials and Physical Methods

All reagents were purchased from Sigma-Aldrich and used as received. Solvents were analytical grade and used without purification. Human cervical cancer cells of HeLa cell line were procured from National Center for Cell Science, Pune, India, and used throughout the study. Elemental (C, H and N) analyses were performed on a Perkin-Elmer 2400 II analyzer. IR spectra were recorded in the region 400–4000 cm^{-1} on a Bruker-Optics Alpha–T spectrophotometer with samples as KBr disks. Electronic spectra were obtained by using a Hitachi U-3501 spectrophotometer. Luminescence property was measured using LS-55 Perkin Elmer fluorescence spectrophotometer at room temperature (298 K) by 1 cm path length quartz cell. Fluorescence images of HeLa cells were taken by a fluorescence microscope (Model: LEICA DMLS) with an objective lens of 20X magnification. THERMO MULTI SCAN EX microplate reader was used to measure the absorbance of culture plate.

Biological Study

Cells were cultured in DMEM (Gibco BRL) supplemented with 10 % FBS (Gibco BRL) and 1 % antibiotic mixture containing PSN (Gibco BRL) at 37 °C in a humidified incubator with 5 % CO_2 flow and cells were grown to 80–90 % confluence, harvested with 0.025 % trypsin (Gibco BRL) and 0.52 mM EDTA (Gibco BRL) in phosphate-buffered saline (PBS), plated at the desired cell concentration and allowed to re-equilibrate for 24 h before any treatment. Cells were rinsed

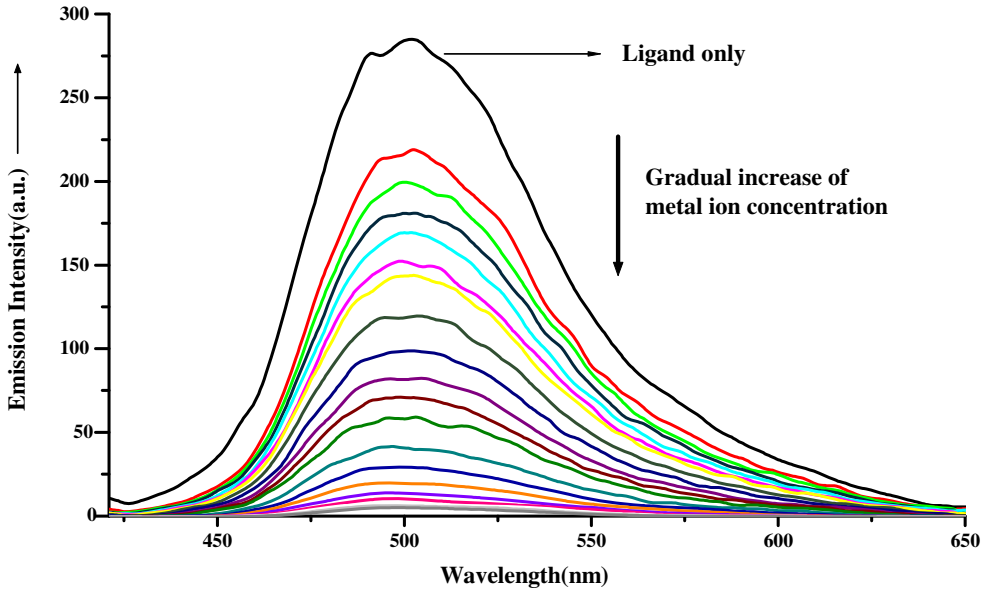

Fig. 4 Fluorescence responses of **HL** (10^{-4} M) to different concentration of Cu^{2+} (0–8 equiv.). The arrow indicates the signal changes as increasing the Cu^{2+} concentration. λ_{ex}=411 nm, λ_{em}=500 nm

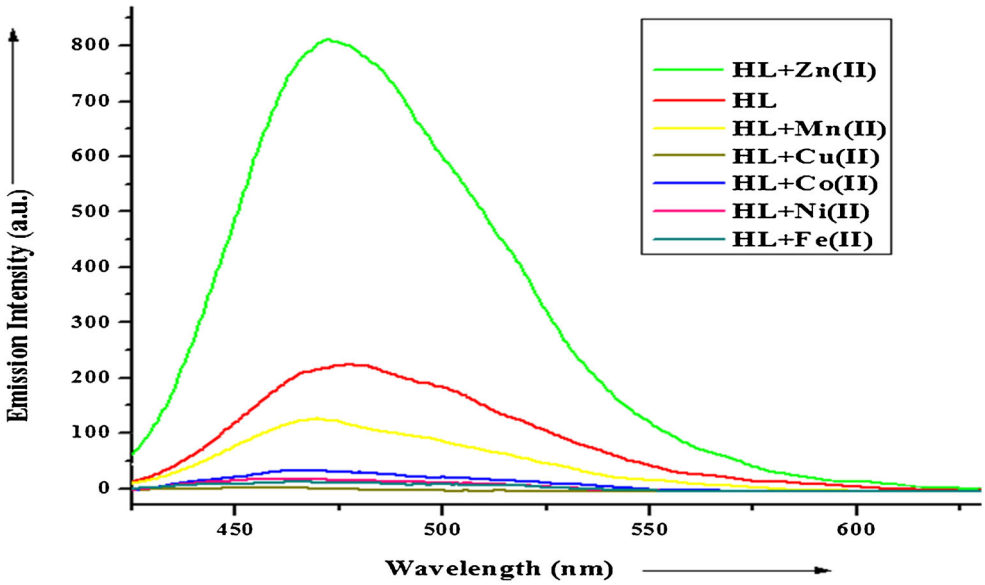

Fig. 5 Fluorescence response of **HL** (10^{-4} M) on addition of various metal ions (conc. of Mn^{2+}, Fe^{2+}, Co^{2+}, Ni^{2+} and $Cu^{2+}=10^{-4}$ M; $[Zn^{2+}]=10^{-6}$ M. λ_{ex}=411 nm

with PBS and incubated with DMEM containing **HL** making the final concentration up to 10 μM in DMEM [the stock solution (1 mM) was prepared by dissolving **HL** in ethanol] for 30 min at 37 °C. After incubation, bright field and fluorescence images of HeLa cells were taken by fluorescence microscope with an objective lens of 20X magnification; fluorescence images of HeLa cells incubated with 10 μM **HL** for 30 min followed by addition of 10 μM Cu^{2+} ion were taken and consequently fluorescence images were taken after further addition of 50 μM Cu^{2+} ion.

In order to test the cytotoxicity of **HL**, 3-(4, 5-dimethylthiazol-2-yl)-2,S-diphenyltetrazolium bromide (MTT) assay was performed as per the procedure described earlier [65]. After treatment with **HL** at different doses of 1, 10, 20, 50 and 100 μM, respectively, for 12 h, 10 μl of MTT solution (10 mg/ml PBS) was added to each well of a 96-well culture plate and again incubated continuously at 37 °C for a period of 3 h. All media were removed from wells and 100 μl of acidic isopropyl alcohol was added into each well. The intracellular formazan crystals (blue-violet) formed were solubilised with 0.04 N acidic isopropyl alcohol and absorbance of the solution was measured at 595 nm wavelength with a microplate reader. The cell viability was expressed as the optical density ratio of the treatment to control. Values were expressed as mean±standard errors of three independent experiments. The cell cytotoxicity was calculated as % cell cytotoxicity= 100 % - % cell viability.

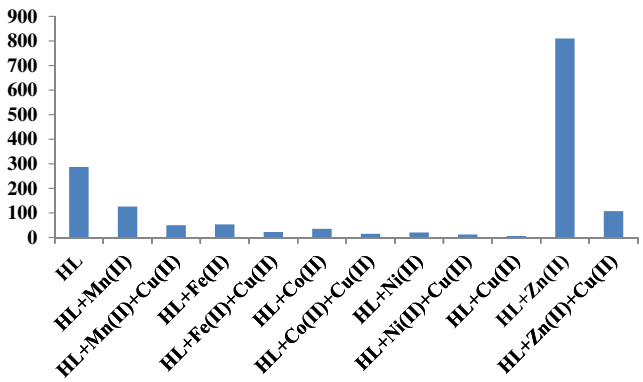

Fig. 6 Competitive fluorescence response of **HL** (10^{-4} M) in presence of 8 equivalent of Cu^{2+} and 8 equivalent of other metal ions in methanol

Synthesis of HL

The chemosensor molecule **HL** was synthesized by following procedure. Pyridoxal hydrochloride (0.406 g, 2 mM) was dissolved in absolute methanol (15 mL) in the presence of KOH (0.112 g, 2 mM) with stirring. After 1 h of stirring, the separated white solid (KCl) was filtered and the obtained clear solution was added to a solution of N,N-dimethylethylenediamine (0.176 g, 2 mM) in methanol (15 mL) with stirring and the resulting reaction mixture was refluxed for 4 h. The completeness of the condensation reaction was checked by performing thin layer chromatography. The solution was evaporated by rotary evaporator and sticky mass obtained was washed by cold ether and dried under vacuum. (Yield: 0.355 g, 0.75 %). ^{1}H NMR (300 MHz, $CDCl_3$): δ 8.90 (s, 1H), 7.74 (s, 1H), 4.72 (s,1H), 3.78 (t, 2H), 3.42 (s, 1H), 2.69 (t, 2H), 2.46 (s, 3H), 2.30 (s, 6H). ^{13}C NMR (75 MHz, $CDCl_3$): δ 18.60, 45.43, 57.35, 59.36, 60.06, 119.66, 131.53, 137.26, 150.50, 155.20, 163.33; Anal. calc. for $C_{12}H_{19}N_3O_2$: C, 60.74; H, 8.07; N, 17.71. Found: C, 59.97; H, 7.79; N, 17.05 %.

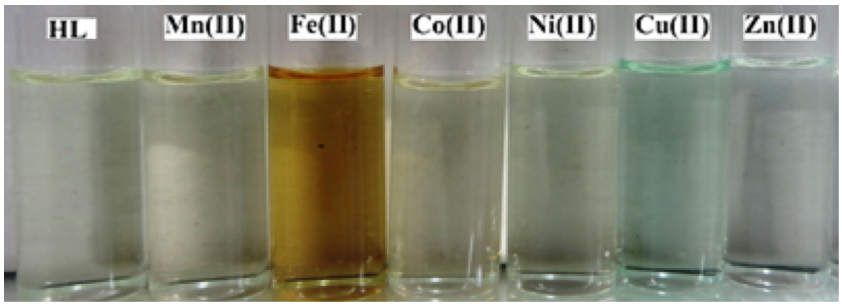

Fig. 7 Colour changes of **HL** upon addition of various metal ions under visible light in MeOH solution

Result and Discussion

Synthesis of Ligand HL

The Schiff base ligand **HL** was synthesized by condensing pyridoxal hydrochloride with N,N-dimethylethylenediamine under reflux in MeOH and characterized by ^{1}H NMR, ^{13}C NMR and FTIR spectroscopy (Fig. 1). The schematic representation of the preparation of the Schiff base ligand **HL** and its copper complexes is given in Scheme 1.

Spectroscopic Characterization

^{1}H NMR Spectral Study of Ligand

The azomethine proton is the sharp singlets at 8.90 ppm. A sharp singlet at 7.75 ppm is assigned as the proton at the ortho position with respect to nitrogen atom of pyridine ring. Another sharp singlet at 4.72 ppm is assigned as the proton attached with carbon atom of $–CH_2OH$ moiety. A triplet at 3.78 is assigned as the two protons attached with carbon atom which is further attached with azomethine nitrogen atom. Another sharp singlet at 3.42 ppm is assigned as the proton attached with oxygen atom of $–CH_2OH$ moiety. Another triplet at 2.69 ppm is assigned as the two protons attached carbon atom near to tertiary nitrogen atom of amine part. A strong sharp singlet at the region 2.45 ppm is due to three protons of $–CH_3$ attached at the ortho position with respect to nitrogen atom of pyridine ring. For **HL**, we get a sharp singlet at 2.30 ppm for the two methyl hydrogen of end nitrogen of amine part. But peaks for phenolic proton is absent probably due to rapid exchange of deuterium of $CDCl_3$.

FTIR Spectroscopy

FTIR spectra of **HL** showed the characteristic band due to $\nu(C{=}N)$ at 1650 cm^{-1}. A broad band of high intensity at 3399 cm^{-1} is attributed to the –OH stretching vibration of the $–CH_2OH$ of the pyridoxal part of the ligand.

UV–vis Spectroscopic Studies

Initially, we have tried to carry out the experiments in water but the solution of **HL** did not show stability over time. Then we extended the experiments in EtOH-H_2O (4:1 *v*/*v*) and methanol solutions. Here, we have reported

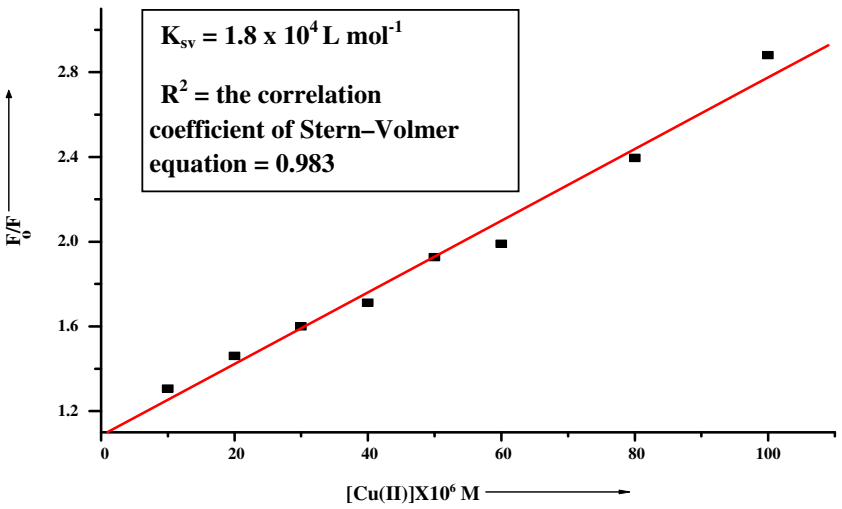

Fig. 8 Stern–Volmer plot of fluorescence quenching of **HL** by Cu^{2+} in methanol

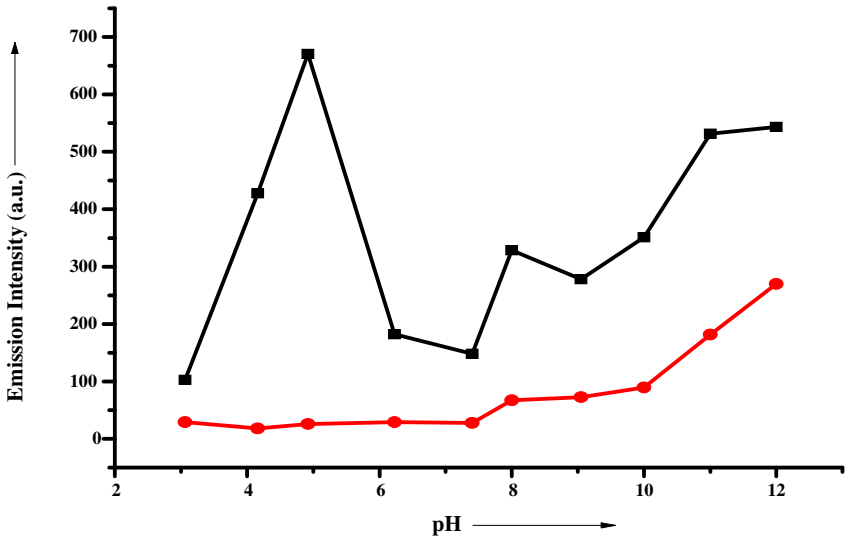

Fig. 9 **The** pH effects on the fluorescence intensity of the free **HL** (0.1 μM) (black, ■) and toward Cu^{2+} anion (300 μM) (red, ●)

the electronic absorption spectral study in UV grade methanol (Fig. 2). In case of **HL**, the absorption bands around 209, 251 and 334 nm are assigned to the π–π* transitions involving imine moiety. The absorption bands at 411 nm is attributed to the n–π* transitions of azomethine group [52].

Figure 3 shows the spectra recorded on titrating 10^{-4} (M) **HL** in methanol with 0.5 (M) Cu^{2+} solution. As evident from Fig. 3, **HL** was characterised by a broad absorption band near the region of 260 nm and 327 nm which can be attributed to the π–π* transitions. Upon stepwise increase in concentration of Cu^{2+}, the absorption intensity at λ_{max}=260 and 327 nm decreased and a new band at 640 nm appeared which was due to d-d transition. In addition, there was an well defined isosbestic point at 467 nm indicating that a stable complex resulted having a certain stoichiometric ratio as found in the previously reported two copper(II) complexes of **HL** [66].

Fluorescence Quenching Properties and Binding Behaviour

The fluorescence spectra of **HL** were obtained by excitation of the fluorophore at 411 nm in methanol. In the absence of metal ion, a strong emission peak was observed at 500 nm. The data were recorded 1 m after copper ion was added. Upon addition of 8 equiv. of Cu^{2+} to the solution of **HL** in methanol, complete quenching was observed (Fig. 4). We initially studied the fluorescence responses of **HL** to different metal ions. For example, the fluorescence spectral outcome of **HL** in the presence of Mn^{2+}, Fe^{2+}, Co^{2+}, Ni^{2+}, Cu^{2+}, Zn^{2+} was measured in methanol. It was found that, when 0.1 equiv. of Cu^{2+} was added to the solution of **HL**, fluorescence quenching was

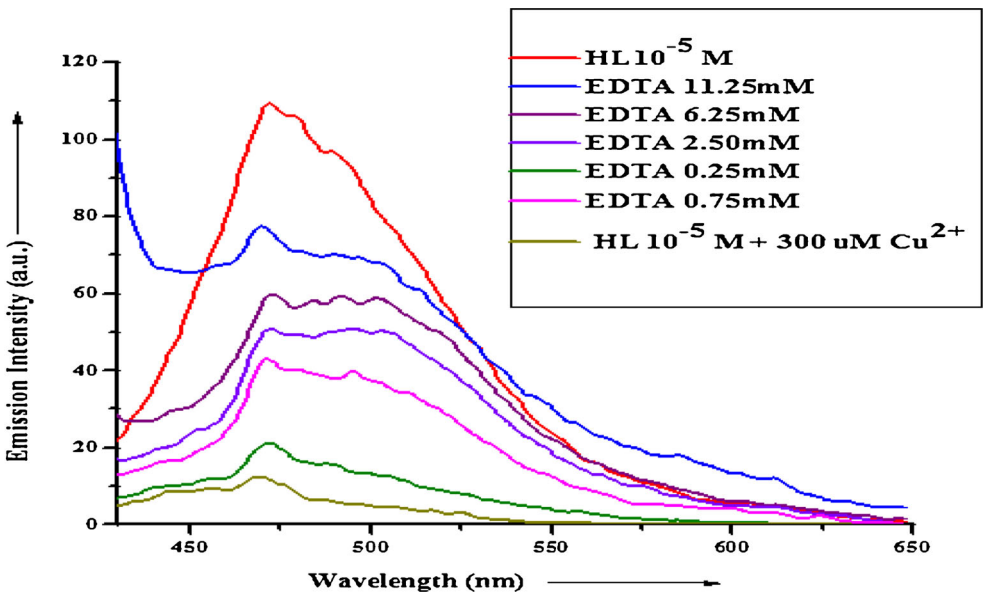

Fig. 10 Fluorescence titration of HL+Cu^{2+} complex with EDTA in methanol:water =9:1 (*v*/*v*) at 25 °C (λ_{ex}=411 nm). Intensity gradually increases upon gradual addition of EDTA (total 11.25 mM) solution

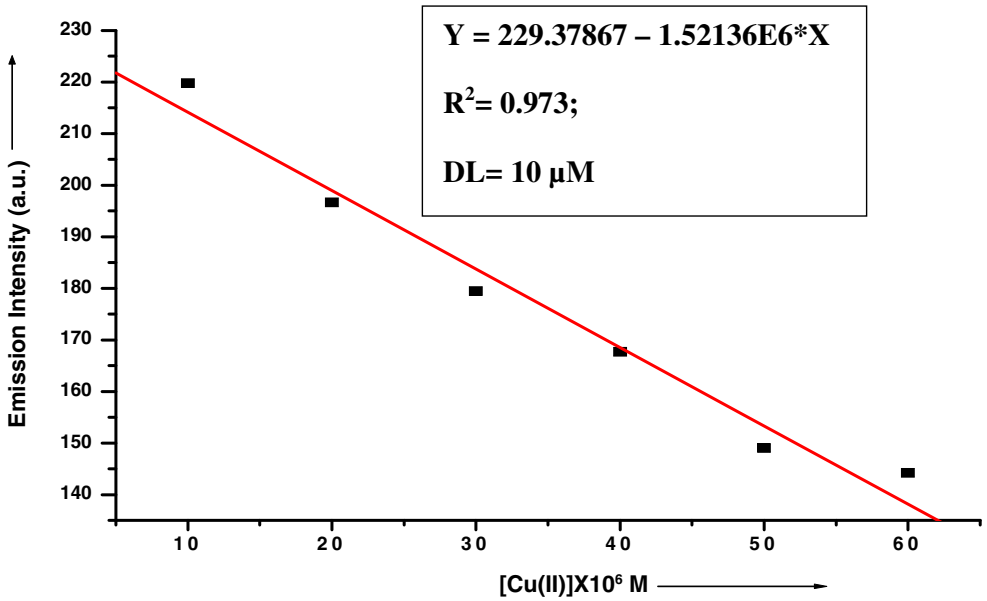

Fig. 11 Plot of emission intensity vs. Cu^{2+} concentration for calculation of detection limit

observed and at 1:1 stoichiometry the quenching efficiency $[(I_0-I)/I_0\times100=47\ \%]$ suggesting that **HL** shows a specific response to Cu^{2+} ions due to the chelation-enhanced fluorescence quenching (CHEQ) effect [67] but was slightly influenced by Mn^{2+}, Fe^{2+}, Co^{2+}, Ni^{2+} ions and highly enhanced by Zn^{2+} ion (Fig. 5).

The selectivity studies of **HL** towards Cu^{2+} over other metal ions are carried out by adding 8 equivalent of Cu^{2+} to the solution of **HL** (0.5×10^{-4} M) in the presence of 8 equivalents of other metal ions. The results indicated that the probe can detect Cu^{2+} with moderate selectivity (Fig. 6).

The fluorescence titration of **HL** with Cu^{2+} was carried out in a methanol solution at 298 K (Fig. 4). The fluorescence intensity of **HL** at 500 nm was consistently reduced when the concentration of Cu^{2+} was increased from 0 to 400 μM. Fluorescence intensity was quenched about 47 % while the concentration of Cu^{2+} reached about 0.1 equivalent. The linear relationship of the fluorescence titration showed that **HL** responded to Cu^{2+} in 1:1 stoichiometry as evident from the crystal structure [66]. The association constant for Cu^{2+} was estimated to be 6.21×10^4 M^{-1} in methanol by the linear Benesi-Hildebrand equation $F_0/(F-F_0)=F_0/[\mathbf{HL}]+F_0/[\mathbf{HL}]\times K_a\times[Cu^{2+}]$ [68] where, F is the change in the fluorescence intensity of **HL** at 500 nm, K_a is the association constant, and [**HL**] and $[Cu^{2+}]$ are the concentration of **HL** and Cu^{2+}, respectively. By plotting $F_0/(F-F_0)$ against the reciprocal of the concentration of Cu^{2+}, the association constant value K_a is obtained from the ratio intercept/slope with a good linear correlation coefficient (R^2=0.9983). The high association constant value is in accordance with the very stable isolated complexes **1** and **2** [66]. Recently, Hou et al., Liu et al. and Wu et al. have reported fluorescein, quinoline and pyrene based effective Cu^{2+} quenching fluorescent sensors that exhibited similar outcome [69–71].

The change in colour of **HL** upon addition of Cu^{2+} was clearly distinguishable from Mn^{2+}, Fe^{2+}, Co^{2+}, Ni^{2+}, Zn^{2+} ions under visible light by the naked-eye (Fig. 7).

From the steady-state Stern-Volmer plot ($K_{sv}=1.8\times10^4$ L mol^{-1}, R^2=0.9834) (Fig. 8) and the linear nature of the plot suggests that only static quenching mode is present.

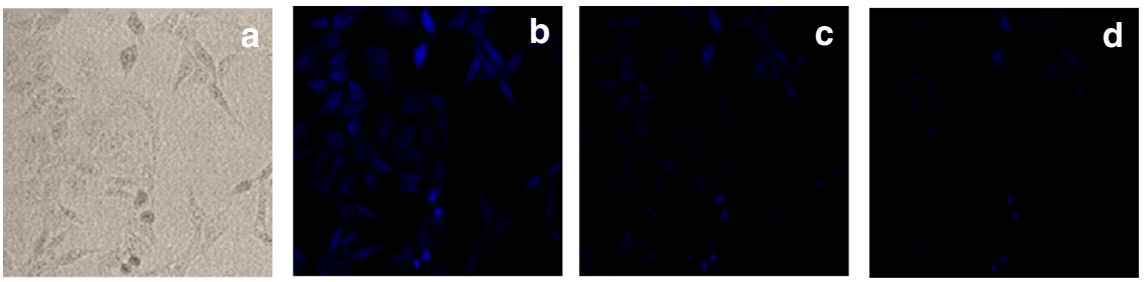

Fig. 12 **a** Phase contrast image of HeLa cells, **b** fluorescence image of HeLa cells, after being incubated with 10 μM **HL** only for 30 min at 37 °C, **c** fluorescence image of HeLa cells after being incubated with 10 μM **HL** for 30 min followed by 10 min incubation with 10 μM extracellular Cu^{2+} ion at 37 °C and **d** reduction of fluorescence intensity in the HeLa cells treated with the sensor and excess Cu^{2+} ion (50 μM). All the samples were excited at 400–450 nm

It is well documented that heavy metal ions such as Cu^{2+}, Cd^{2+}, Hg^{2+} and Pb^{2+} tend to quench the fluorescence through electron- and/or energy-transfer processes [72].

From the pH dependence of fluorescence study (Fig. 9), it was found that the fluorescence intensity of **HL** at 494 nm remains unaffected at pH 7.4 which makes it suitable for application under physiological conditions. These results indicate that **HL** can be used as a selective fluorescent probe to recognize and distinguish Cu^{2+} in the presence of various metal ions. We have also performed a reversibility experiment which proved that the binding of Cu^{2+} to **HL** is reversible which is the key requirement of an ideal biologically relevant chemosensor so that binding of guest molecule must occur reversibly. In the presence of EDTA, a strong chelating ligand, due to its strong affinity towards Cu^{2+}, decomposition of the Cu complex of **HL** takes place thereby giving enhancement of the fluorescent emission at 472 nm. As shown in Fig. 10 after the addition of EDTA, the emission intensity of the original ligand was gradually restored. This phenomenon certainly gives a tacit support towards the reversible binding of **HL** with Cu^{2+}.

Determination of Detection Limit

To determine the detection limit, following equation was used.

$$\mathbf{DL} = \mathbf{K} \times \mathbf{Sb} \Big/ \mathbf{S}$$

where K=2 or 3 (we take 3 in this case), Sb is the standard deviation of the blank solution and S is the slope of the calibration curve. Here, the detection limit of **HL** for Cu^{2+} was determined as 10 μM (Fig. 11).

Cell Studies

The intracellular Cu^{2+} imaging behaviour of **HL** was studied on HeLa cells with the aid of fluorescence microscopy. After incubation with **HL** the cells displayed moderate intracellular fluorescence (Fig. 12b). However, fluorescence intensity was gradually decreased when the **HL** pre-incubated cells were added with Cu^{2+} ion (10–50 μM) (Fig. 12c and d). Therefore this provides confirmatory evidence of this sensor to have the specific ability to sense Cu^{2+} ions. The emission responses of **HL** with various concentrations of added Cu^{2+} are clearly evident from the cellular imaging. Hence, these results indicate that **HL** is an efficient candidate for monitoring changes in the intracellular Cu^{2+} concentration under different biological conditions. In order to test its cytotoxicity, we performed MTT assay in human cervical cancer cells treated with various concentrations of chemosensor **HL** for up to 3 h. As shown in Fig. 12a, 10 μM **HL** did not show significant cytotoxic effects on human cervical cancer cells for at least up to 12 h of its treatment. This thus suggests that **HL** can be readily used for cellular application at the indicated dose and time of incubation without much concern about its cytotoxicity (Fig. 13).

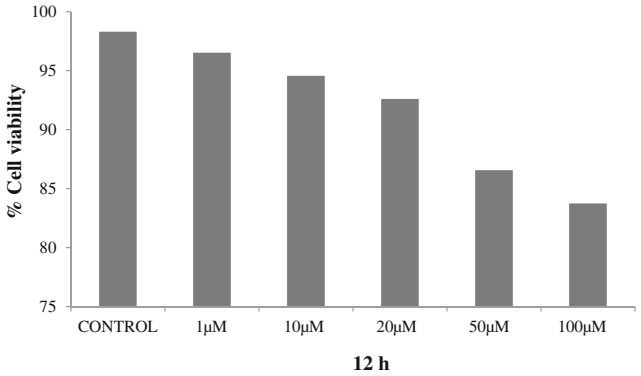

Fig. 13 Representation of % cell viability of HeLa cells treated with different concentrations (1–100 μM) of **HL** for 12 h determined by MTT assay. Results are expressed as mean of three independent experiments

Conclusion

A new fluorescent probe **HL** based on pyridoxal fluorophore has been synthesized for detecting Cu^{2+} ion with moderate selectivity in methanol with a low detection limit of 10 μM. **HL** has appreciable sensing response at physiological pH and the process is found to be reversible when tested with EDTA, indicating that the sensor is promising for biological applications.

Acknowledgments Financial support from the University Grants Commission for senior research fellowship to S. Mandal [Sanction No. UGC/847/Jr. Fellow (Upgradation)] is gratefully acknowledged. SKM is grateful to DST-PURSE PROGRAMME for partial financial support of the biological work.

References

1. Gaggelli E, Kozlowski H, Valensin D, Valensin G (2006) Copper homeostasis and neurodegenerative disorders (Alzheimer's, prion, and Parkinson's diseases and amyotrophic lateral sclerosis. Chem Rev 106:1995–2044
2. Que EL, Domaille DW, Chang CJ (2008) Metals in neurobiology: probing their chemistry and biology with molecular imaging. Chem Rev 108:1517–1549
3. Radisky D, Kaplan J (1999) Regulation of transition metal transport across the yeast plasma membrane. J Biol Chem 274:4481–4484
4. Chan YH, Chen J, Liu Q, Wark SE, Son DH, Batteas JD (2010) Ultrasensitive copper(II) detection using plasmon-enhanced and photo-brightened luminescence of CdSe quantum dots. Anal Chem 82:3671–3678
5. Multhaup G, Schlicksupp A, Hesse L, Beher D, Ruppert T, Masters CL, Beyreuther K (1996) The amyloid precursor protein of Alzheimer's disease in the reduction of copper(II) to copper(I). Science 271:1406–1409

6. Lovstad RA (2004) A kinetic study on the distribution of Cu(II)-ions between albumin and transferrin. BioMetals 17:111–113
7. World Health Organization (2011) Guidelines for drinking-water quality
8. Bings NH, Bogaerts A, Broekaert JAC (2008) Anal Chem 80: 4317–4347
9. Siripinyanond A, Worapanyanond S, Shiowatana J (2005) Field-flow fractionation-inductively coupled plasma mass spectrometry: an alternative approach to investigate metal-humic substances interaction. Environ Sci Technol 39:3295–3301
10. Tanyanyiwa J, Hauser PC (2002) High-voltage contactless conductivity detection of metal ions in capillary electrophoresis. Electrophoresis 23:3781–3786
11. Xiang Y, Tong AJ, Jin PY, Ju Y (2006) New fluorescent rhodamine hydrazone chemosensor for Cu(II) with high selectivity and sensitivity. Org Lett 8:2863–2866
12. Huang CC, Yang Z, Lee KH, Chang HT (2007) Synthesis of highly fluorescent gold nanoparticles for sensing mercury(II). Angew Chem Int Ed 46:6824–6828
13. Sirilaksanapong S, Sukwattanasinitt M, Rashatasakhon P (2012) 1, 3,5-Triphenylbenzene fluorophore as a selective Cu^{2+} sensor in aqueous media. Chem Commun 48:293–295
14. Huang L, Cheng J, Xie KF, Xi PX, Hou FP, Li ZP, Xie GQ, Shi YJ, Liu HY, Bai DC, Zeng ZZ (2011) Cu(2+)-selective fluorescent chemosensor based on coumarin and its application in bioimaging. Dalton Trans 40:10815–10817
15. Wampler JE, Churchich JE (1969) Phosphorescence of pyridoxal. J Biol Chem 244:1477–1480
16. Eliot AC, Kirsch JF (2004) Pyridoxal phosphate enzymes: mechanistic, structural, and evolutionary considerations. Annu Rev Biochem 73:383–415
17. John RA (1995) Pyridoxal phosphate-dependent enzymes. Biochim Biophys Acta 1248:81–96
18. Toney MD (2005) Reaction specificity in pyridoxal phosphate enzymes. Arch Biochem Biophys 433:279–287
19. Christen P, Metzler DE (1985) Transaminases. Wiley, New York
20. Hayashi H, Mizuguchi H, Miyahara I, Islam MM, Ikushiro H, Nakajima Y, Hirotsu K, Kagamiyama H (2003) Strain and catalysis in aspartate aminotransferase. Biochim Biophys Acta 1647:103–109
21. Liu W, Peterson PE, Langston JA, Jin X, Zhou X, Fisher AJ, Toney MD (2005) Kinetic and crystallographic analysis of active site mutants of Escherichia coli gamma-aminobutyrate aminotransferase. Biochemistry 44:2982–2992
22. Fogle EJ, Liu W, Woon ST, Keller JW, Toney MD (2005) Role of Q52 in catalysis of decarboxylation and transamination in dialkylglycine decarboxylase. Biochemistry 44:16392–16404
23. Sun S, Toney MD (1999) Evidence for a two-base mechanism involving tyrosine-265 from arginine-219 mutants of alanine racemase. Biochemistry 38:4058–4065
24. Watanabe A, Yoshimura T, Mikami B, Hayashi H, Kagamiyama H, Esak NJ (2002) Reaction mechanism of alanine racemase from bacillus stearothermophilus: X-ray crystallographic studies of the enzyme bound with n-(5′-phosphopyridoxyl)alanine. Biol Chem 277:19166–19172
25. Major DT, Gao J (2006) A combined quantum mechanical and molecular mechanical study of the reaction mechanism and alpha-amino acidity in alanine racemase. J Am Chem Soc 128:16345–16357
26. Schirch V, Szebenyi DME (2005) Serine hydroxymethyltransferase revisited. Curr Opin Chem Biol 9:482–487
27. Paiardini A, Contestabile R, Aguanno SD, Pascarella S, Bossa F (2003) Threonine aldolase and alanine racemase: novel examples of convergent evolution in the superfamily of vitamin B_6-dependent enzymes. Biochim Biophys Acta 1647:214–219
28. Brazeau BJ, Johnso BJ, Wilmot CM (2004) Copper-containing amine oxidases. Biogenesis and catalysis; a structural perspective. Arch Biochem Biophys 428:22–31
29. Mure M, Mills SA, Klinman JP (2002) Catalytic mechanism of the topa quinone containing copper amine oxidases. Biochemistry 41: 9269–9278
30. Smith AT, Majtan T, Freeman KM, Su Y, Kraus JP, Burstyn JN (2011) Cobalt cystathionine β-synthase: a cobalt-substituted heme protein with a unique thiolate ligation motif. Inorg Chem 50:4417–27
31. Prior FGR (1985) Theoretical involvement of vitamin B_6 in tumour initiation. Med Hypotheses 16:421–428
32. Bender DA, Bowden JF, Coulsen WF, Dewji MR, Sutton J, Symes EK (1988) Current topics in nutrition and disease: clinical and physiological applications of vitamin B_6, New York, U.S.A.
33. Snell EE (1945) The vitamin B_6 group. V. The reversible interconversion of pyridoxal and pyridoxamine by transamination reactions. J Am Chem Soc 67:194–197
34. Guirard BM, Snell EE (1981) In: Florkin M, Stotz EH (eds) Comprehensive Biochemistry. Elsevier, Amsterdam
35. Mehansho H, Henderson LM (1980) Transport and accumulation of pyridoxine and pyridoxal by erythrocytes. J Biol Chem 255: 11901–11907
36. Casella L, Gullotti M (1983) Coordination modes of histidine. 6. Transamination in the 2-formylpyridine-amino acid-metal ion systems. Stereochemistry of zinc(II) and copper(II) complexes of N-(2-pyridylmethylidene)amino acids. Inorg Chem 22:2259–2266
37. Walsh C (1978) Chemical approaches to the study of enzymes catalyzing redox transformations. Annu Rev Biochem 47:881–931
38. Vederas JC, Floss HG (1980) Stereochemistry of pyridoxal phosphate catalyzed enzyme reactions. Acc Chem Res 13:455–463, **and references therein**
39. Walsh C, Pascal RA, Johnson M, Raines R, Dikshit D, Krantz A, Honna M (1981) Mechanistic studies on the pyridoxal phosphate enzyme 1-aminocyclopropane-1-carboxylate deaminase from Pseudomonas sp. Biochemistry 20:7509–7519
40. Koh LL, Ranford JO, Robinson WT, Svensson JO, Tan ALC, Wu D (1996) Model for the reduced schiff base intermediate between amino acids and pyridoxal: copper(II) complexes of N-(2-hydroxybenzyl)amino acids with nonpolar side chains and the crystal structures of [Cu(N-(2-hydroxybenzyl)-D,L-alanine)(phen)].H_2O and [Cu(N-(2-hydroxybenzyl)-D,L-alanine)(imidazole)]. Inorg Chem 35: 6466–6472
41. Metzler DE, Longenecker JB, Snell EE (1953) Reversible catalytic cleavage of hydroxyamino acids by pyridoxal and metal salts. J Am Chem Soc 75:2786–2787
42. Metzler DE, Olivard J, Snell EE (1954) Transamination of pyridoxamine and amino acids with glyoxylic acid. J Am Chem Soc 76: 644–648
43. Metzler DE, Snell EE (1952) Some transamination reactions involving vitamin B_6. J Am Chem Soc 74:979–983
44. Longenecker JB, Snell EE (1957) The comparative activities of metal ions in promoting pyridoxal-catalyzed reactions of amino acids. J Am Chem Soc 79:142–145
45. Matsushima Y, Martell AE (1967) Pyridoxal analogs. IX. Electron absorption spectra and molecular species in methanol solution. J Am Chem Soc 89:1322–1330
46. Abbott EH, Martell AE (1969) Nuclear magnetic resonance investigation of the metal ion and proton-catalyzed reaction of some vitamin B_6 Schiff bases. J Am Chem Soc 91:6931–6939
47. Wagner MR, Walker FA (1983) Spectroscopic study of 1:1 copper(II) complexes with Schiff base ligands derived from

salicylaldehyde and L-histidine and its analogs. Inorg Chem 22:3021–3028
48. Snell EE, Braunstein AE, Severin ES, Torchinsky YM (1968) Eds. Pyridoxal Catalysis: Enzymes and Model Systems; Interscience: NewYork
49. Holm RH (1973) In: Eichhorn GL (ed) Inorganic biochemistry. Elsevier, New York
50. Martell AE (1973) In: Sigel H (ed) Metal ions in biological systems, vol 2. Dekker, New York
51. Naskar S, Naskar S, Butcher RJ, Chattopadhyay SK (2010) Synthesis, X-ray crystal structures and spectroscopic properties of two Ni (II) complexes of pyridoxal Schiff's bases with diamines: Importance of steric factor in stabilization of water helices in the lattices of metal complex. Inorg Chim Acta 363:404–411
52. Naskar S, Naskar S, Figgie HM, Sheldrick WS, Chattopadhyay SK (2010) Synthesis, crystal structures and spectroscopic properties of two Zn(II) Schiff's base complexes of pyridoxal. Polyhedron 29: 493–499
53. Abbott EH, Martell AE (1970) Mechanism of formation, structure, stereochemistry, and racemization of bis[pyridoxylidene(amino acidato)]aluminum(III) complexes. J Am Chem Soc 92:5845–5851
54. Martell AE, Eidson AF (1975) Absorption and circular dichroism spectra of the pyridoxylidenalanatoaluminum (III) complex. Bioinorg Chem 4:277–289
55. Capasso S, Giordano F, Mattia C, Mazzarella L, Ripamonti A (1974) Stereochemistry of model compounds for pyridoxal-catalysed reactions. Crystal structures of the hydrated complexes bis(pyridoxylidene-DL-valinato)nickel(II) and bis(pyridoxylidene-L-valinato)zinc(II). J Chem Soc Dalton Trans 2228–2233
56. Pessoa CJ, Cavaco I, Correia I, Duarte MT, Gillard RD, Henriques RT, Higes FJ, Madeira C, Tomaz I (1999) Preparation and characterisation of new oxovanadium(IV) Schiff base complexes derived from amino acids and aromatic o-hydroxyaldehydes. Inorg Chim Acta 293:1–11
57. Shanbhag VM, Martell AE (1990) Schiff bases of pyridoxal 5′-phosphate and 5′-deoxypyridoxal with phenylglycine derivatives and their metal complexes. Inorg Chem 29:1023–1031
58. Correia I, Pessoa CJ, Duarte MT, Henriques RT, Piedade MFM, Veiros LF, Jakusch T, Kiss T, Dörnyei Á, Castro MMCA, Geraldes CFGC, Avecilla F (2004) N, N'-Ethylenebis(pyridoxylideneiminato) and N, N'-Ethylenebis(pyridoxylaminato): Synthesis, Characterization, Potentiometric, Spectroscopic, and DFT Studies of Their Vanadium(IV) and Vanadium(V) Complexes. Chem Eur J 10: 2301–2317
59. Correia I, Dörnyei Á, Avecilla F, Kiss T, Pessoa CJ (2006) X-ray crystal structure and characterization in aqueous solution of {N, N-ethylenebis(pyridoxylaminato)}zinc(II). Eur J Inorg Chem 3:656–662
60. Sundaravel K, Suresh E, Palaniandavar M (2009) Synthesis, structures, spectral and electrochemical properties of copper(II) complexes of sterically hindered Schiff base ligands. Inorg Chim Acta 362:199–207
61. Adao P, Maurya MR, Kumar U, Avecilla F, Henriques RT, Kusnetsov ML, Pessoa CJ, Correia I (2009) Vanadium-salen and -salan complexes: characterization and application in oxygen transfer reactions. Pure Appl Chem 81:1279–1296
62. Mukherjee T, Pessoa JC, Kumar A, Sarkar AR (2011) Oxidovanadium(IV) schiff base complex derived from vitamin B_6: synthesis, characterization, and insulin enhancing properties. Inorg Chem 50:4349–4361
63. Mauryaa MR, Bishta M, Avecilla F (2011) Synthesis, characterization and catalytic activities of vanadium complexes containing ONN donor ligand derived from 2-aminoethylpyridine. J Mol Catal A Chem 344:18–27
64. Mandal S, Modak R, Goswami S (2013) Synthesis and characterization of a copper(II) complex of a ONN donor schiff base ligand derived from pyridoxal and 2-(pyrid-2-yl)ethylamine – a novel pyridoxal based fluorescent probe. J Mol Struct 1037:352–360
65. Mossman T (1983) Rapid colorimetric assay for cellular growth and survival. J Immunol Methods 65:55–63
66. Mandal S, Naskar B, Modak R, Sikdar Y, Chatterjee S, Biswas S, Mondal Kumar T, Modak D, Goswami S (2015) Syntheses, crystal structures, spectral study and DFT calculation of three new copper(II) complexes derived from pyridoxal hydrochloride, N, N-dimethylethylenediamine and N, N- diethylethylenediamine. J Mol Struct 1088:38–49
67. Swamy KMK, Kim HN, Soh JH, Kim Y, Kim SJ, Yoon J (2009) Manipulation of fluorescent and colorimetric changes of fluorescein derivatives and applications for sensing silver ions. Chem Commun 1234–1236
68. Benesi HA, Hildebrand JH (1949) A spectrophotometric investigation of the interaction of iodine with aromatic hydrocarbons. J Am Chem Soc 71:2703–2707
69. Hou F, Cheng J, Xi P, Chen F, Huang L, Xie G, Shi Y, Liu H, Bai D, Zeng Z (2012) Recognition of copper and hydrogen sulfide in vitro using a fluorescein derivative indicator. Dalton Trans 41:5799–5804
70. Liu Z-C, Yang Z, Li T, Wang B, Li Y, Qin D, Wang M, Yan M (2011) An effective Cu(II) quenching fluorescence sensor in aqueous solution and 1D chain coordination polymer framework. Dalton Trans 40:9370–9373
71. Wu SP, Huang ZM, Liu SR, Chung PK (2012) A pyrene-based highly selective turn-on fluorescent sensor for copper(II) ion and its application in live cell imaging. J Fluoresc 22:253–259
72. Kavallieratos K, Rosenberg JM, Che W–Z, Ren T (2005) Fluorescent sensing and selective Pb(II) extraction by a dansylamide ion-exchanger. J Am Chem Soc 127:6514–6515